

Semiconducting chains of gold and silver

Frederico Fioravante and R. W. Nunes*

*Departamento de Física, Universidade Federal de Minas Gerais,
CP 702, 30123-970, Belo Horizonte, MG, Brazil*

(Dated: November 9, 2018)

The authors introduce a geometry for ultrathin Au and Ag wires that *ab initio* calculations indicate to be more stable than previously considered planar geometries for these systems, by about 0.1 eV per atom. This structure is insulating for both metals and for related $\text{Ag}_{0.5}\text{Au}_{0.5}$ alloys, with gaps of 1.3 eV for Au, 0.8 eV for Ag, and varying between 0.1 eV and 1.9 eV for the alloys. The insulating nature of the geometry is not a result of Peierls instabilities, and is analyzed in terms of an interplay between geometric and electronic structure effects.

PACS numbers: 61.46.Km, 62.23.Hj, 73.22.-f

Nanowires (NWs) based on $4d$ and $5d$ metals are a topic of intense current interest in the physics of nanomaterials. Understanding the connection between atomic structure and transport, in the limit of the ultrathin monoatomic wires that have been produced experimentally, [1, 2] is crucial to the future manipulation of metallic wires and electric contacts in nanoscale electronic devices. Previous experimental and theoretical works on pure and alloy NWs have established that structure and transport are dynamically and strongly linked in the nanoscale limit. [3–7] Detailed investigation of the structural landscape of ultrathin pure and alloy NWs is thus of paramount importance.

Previous theoretical studies [6, 8–12] of infinite monoatomic Au and Ag NWs have considered two planar zigzag configurations, with angles between two noncollinear bonds along the chain of $\sim 60^\circ$ [see Fig. 1(b)] and $\sim 130^\circ$, respectively. Both zigzag geometries are stable for Au, while for Ag only the 60° geometry is a minimum of the $E \times \ell$ surface. [10] This difference between Au and Ag has been tied to a stronger relativistic effect in Au, that leads to enhanced sd hybridization and stabilization of the low-coordinated structure, an effect that is also observed in the surface reconstruction of $4d$ and $5d$ metals. [13] For both metals, the zigzag structures remain metallic, and their stability has been connected with a gapless Peierls transition (GPT), where transversal distortions lower the energy, but a gap does not open at the Fermi level. [14] In the recent work of Cheng and collaborators, the pathway of the thinning process of Ag NWs, in mechanical break junction experiments (MBJE), [2–5] is connected to the successive stable minima of the $E \times \ell$ curve, as the NW radius decreases. [15]

In the present work we examine the structure of ultrathin noble-metal NWs. Our calculations indicate the existence of a planar structure for both Ag and Au, and also for $\text{Ag}_{0.5}\text{Au}_{0.5}$ alloys, that has not been addressed in previous studies for these systems. In this geometry, the average coordination remains fourfold, like in the

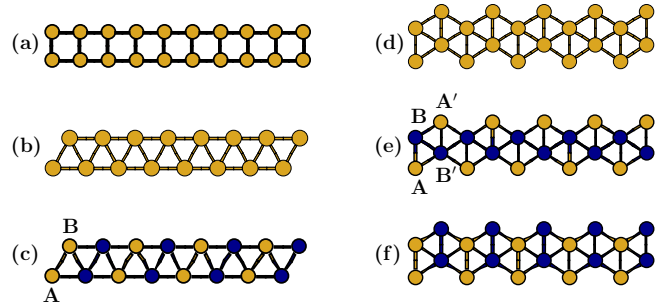


FIG. 1: (Color online) Ag, Au, and $\text{Ag}_{0.5}\text{Au}_{0.5}$ nanowire structures: (a) SQ3; (b) ZZ4; (c) A_1ZZ_4 ; (d) ZZ3+5; (e) A_1ZZ_3+5 ; and (f) A_2ZZ_3+5 . For the alloys, light (yellow online) and dark (blue online) circles represent Au and Ag atoms, respectively.

60° zigzag one, but the four atoms in the unit cell alternate between threefold- and fivefold-coordinated sites, in a double zigzag structure [shown in Figs. 1(d)-(f)] that is lower in energy than the 60° zigzag. Moreover, the structure is insulating, with energy gaps of 1.3 eV and 0.8 eV for Au and Ag, respectively, and does not result from either a Peierls or a GPT instability. Gaps for four possible related alloy geometries vary between 0.1 eV and 1.9 eV. No Peierls instabilities are expected for this structure, given its insulating nature. This is a striking result: the structure, besides being lower in energy than the planar ones considered in previous works, is an equilibrium (unstrained) insulating chain for these atoms, not related to Peierls instabilities, with sizeable energy gaps.

We employ an *ab initio* methodology implemented in the SIESTA package, [16] based on the Kohn-Sham formulation of density functional theory (DFT). [17] The generalized gradient approximation (GGA) [18] is used for the exchange-correlation energy, and norm-conserved Troullier-Martins pseudopotentials [19] represent the ionic cores. Cutoff constrained pseudo-atomic local orbitals form the basis of representation of the electronic wave functions, with energy shifts of ~ 7 mRy. A double-zeta expansion is used for each radial basis function, including polarization orbitals for the ($l = 0$) s functions. In all our calculations, convergence of total energy

*Electronic address: rwnunes@fisica.ufmg.br

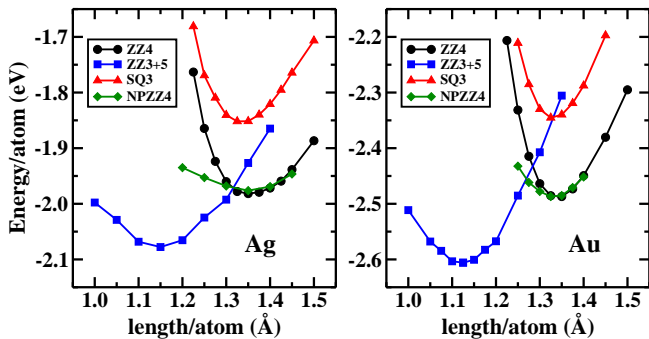


FIG. 2: (Color online) Energy (in eV/atom) \times strain (in $\text{\AA}/\text{atom}$) curves for Au and Ag nanowires in ZZ3+5, ZZ4, NPZZ4, and SQ3 geometries.

differences and atomic forces to within 1 meV/atom and 0.003 eV/ \AA , respectively, was enforced.

The structures of the infinite chains we consider are shown in Fig. 1. (a) shows a planar threefold-coordinated square chain (SQ3). (b) shows the previously-considered 60° planar zigzag fourfold-coordinated chain (ZZ4). (d) shows the planar double-zigzag chain we introduce in this study, with threefold- and fivefold-coordinated atoms (ZZ3+5). The latter is composed of two intercalated subunits, as indicated in Fig. 1(e) by primed and unprimed letters. Sites A and A' (B and B') are both threefold (fivefold) coordinated, and are related by an inversion symmetry in the ideal structure. We considered four alloy structures derived from ZZ3+5, with Au and Ag assigned to A and B sites, as follows. (i) A_1ZZ3+5 [Fig. 1(e)]: Au in A and A' and Ag in B and B'; (ii) A_2ZZ3+5 [Fig. 1(f)]: Au in A and B and Ag in A' and B'; (iii) A_3ZZ3+5 : Au in A and B' and Ag in A' and B; and (iv) A_4ZZ3+5 : Ag in A and A' and Au in the B and B'. In addition, we considered two ZZ4 alloy structures, (i) A_1ZZ4 [Fig. 1(c)]: with Au and Ag atoms alternating on both the A (bottom) and B (top) sites; and (ii) A_2ZZ4 : with Au atoms on the A sites and Ag on the B sites. For all pure systems, we performed calculations at fixed strain (length per atom), with full relaxation of internal degrees of freedom. For the minima of each $E \times \ell$ curve, full relaxation was performed, allowing cell vectors to relax until residual stresses were negligible. For the alloys, we only performed full relaxations to obtain the unstrained minima of the configurations described above.

Figure 2 shows the $E \times \ell$ curves for each geometry, for Au and Ag. All energies are referred to the energy of the isolated atomic components. For Au (Ag), the minimum for the ZZ3+5 geometry is 0.12 (0.09) eV/atom lower in energy than the one for the ZZ4 structure. Among the structures in Fig. 2, the SQ3 geometry shows the highest equilibrium energy for both metals. Our results for the total energies, the equilibrium length, and the electronic band gap, for each structure, are included in Table I. For the ZZ4, our values are in good agreement with previously published results. [6, 8–10, 12]

TABLE I: Energy, length per atom, and electronic band gap (at the level of GGA-DFT) of Au, Ag, and $\text{Ag}_{0.5}\text{Au}_{0.5}$ nanowires, at the equilibrium geometry.

Structure	Energy (eV/atom)	length ($\text{\AA}/\text{atom}$)	Gap (eV)
Ag - SQ3	-1.85	1.34	0.00
Ag - ZZ4	-1.99	1.35	0.00
Ag - ZZ3+5	-2.08	1.14	0.78
Au - SQ3	-2.35	1.33	0.00
Au - ZZ4	-2.49	1.34	0.00
Au - ZZ3+5	-2.61	1.12	1.29
A_1ZZ3+5	-1.88	1.14	1.85
A_2ZZ3+5	-1.77	1.12	0.93
A_3ZZ3+5	-1.74	1.13	1.06
A_4ZZ3+5	-1.69	1.13	0.11
A_1ZZ4	-1.71	1.33	0.59
A_2ZZ4	-1.65	1.34	0.00

Regarding the stability of the ZZ3+5, we believe our results to be relevant in the context of the thinning process of the NWs in MBE, as discussed in Ref. 15, whenever the time scale of this process allows for the stabilization of the successive local minima, as the NW atomic density (and radius) decreases. In the atomic density range we investigate in this work, the ZZ3+5 geometry is the most stable, and should be a “magic structure” (in the language of Ref. 15) adopted by the NW in the thinning process. We can also look at the NW stability issue from the other end, i.e., at the ultrathin limit, by identifying possible transitions between locally stable NW structures, as the applied tension, hence the atomic density, fluctuate. An upper bound for the barrier involved in the ZZ4-to-ZZ3+5 transition is given by the energy difference between the ZZ4 minimum and the crossing of the ZZ4 and ZZ3+5 curves in Fig. 2, plus the barrier for the transformation, when both structures have the length per atom corresponding to the crossing point. In Fig. 2, we also show the $E \times \ell$ curve for a non-planar variation of the ZZ4 geometry (NPZZ4), where small non-planar distortions are allowed. ZZ4 and NPZZ4 are very nearly degenerate at the corresponding minima. Our upper-bound barrier for the ZZ4-to-ZZ3+5 transformation is of the order of the room-temperature thermal energy for Ag (~ 50 meV) and Au (~ 70 meV). In the case of Au, a lower barrier is obtained starting from the NPZZ4, while in Ag a lower-barrier path starts from the ZZ4 itself.

The band structures of the ZZ4 and ZZ3+5 structures for Au and Ag are shown in Fig. 3(a)-(d). In both cases, the Fermi level (E_f) for the ZZ4 geometry does not occur at the $\pi/2a$ vector, and the stability and semiconducting nature of the period-doubling ZZ3+5 does not result from either a GPT or a Peierls instability. It derives, rather, from intricate band-structure effects, which are different between the two metals. We discuss first the band structure of the ZZ4 geometries. We have analyzed in detail the orbital-projected density of states resulting

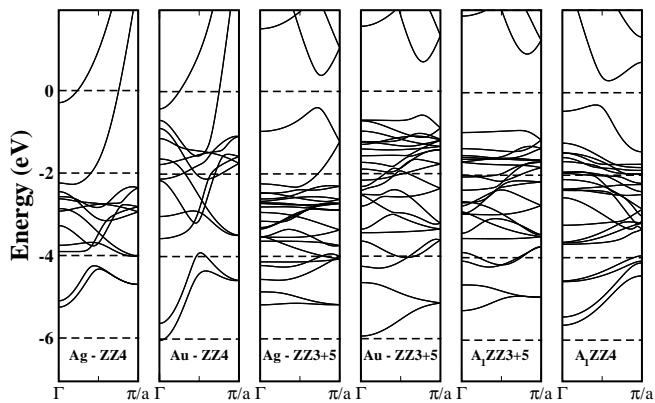


FIG. 3: Energy bands for Au, Ag, and $\text{Ag}_{0.5}\text{Au}_{0.5}$ nanowires in ZZ4 and ZZ3+5 geometries.

from the bands shown in Fig. 3. For both Ag and Au, the two bands crossing E_f are one almost-purely s band, crossing near one quarter of the Brillouin zone, and one hybridized sd band crossing near the point at three quarters of the zone, with predominantly d character. Due to the relativistic effect, the two metals differ in the nature of the hybridized band: s and d levels are more intermixed in the case of Au, while the s levels are higher in energy with respect to d levels, in the case of Ag. This explains the presence of a large pseudo-gap region below the Fermi level in the case of Ag which becomes very small in the case of Au, since the density of states (DOS) of the d -dominant band peaks at much lower energies with respect to the s band in the case of Ag.

In the ZZ3+5 structure, the presence of two sites with different coordinations causes the DOS peaks dominated by the threefold (fivefold) sites to shift upwards (downwards), relative to the ZZ4 peaks. In a tight-binding language, the onsite terms are shifted due the change in coordination. As a result, in the case of Ag, the gap is between two nearly purely s bands (plus the p character from the polarization orbitals). The top of the valence band (HOMO) is a bonding s band from the threefold

atoms while the bottom of the conduction band (LUMO) is an antibonding band from the fivefold atoms. The bonding band from the fivefold sites is deeper in energy than the HOMO, and the antibonding one from the threefold sites is higher than the LUMO. In the case of Au, the HOMO band is a strongly mixed sd band with d character from both types of sites (the fivefold site is dominant), and s character from the threefold sites, while the LUMO is the same as in Ag, the antibonding s band from the fivefold sites.

For the alloys, the most stable $\text{A}_1\text{ZZ3}+5$ has Au in the threefold sites and Ag in the fivefold sites, while in the high-energy $\text{A}_4\text{ZZ3}+5$ Au and Ag switch places. This is due to stronger relativistic effects in Au, that lead to its stronger tendency to form low-coordinated structures. The gaps for these two alloys can be obtained accurately from the HOMO and LUMO of the pure Au and Ag structures. Since HOMO bands are dominated by threefold sites and LUMO ones by fivefold sites, and HOMO and LUMO energies are deeper in Au than in Ag, a larger gap is expected for $\text{A}_1\text{ZZ3}+5$, with Au at threefold sites leading to a deeper HOMO, and Ag at fivefold sites leading to a higher LUMO. The opposite effect would occur in $\text{A}_4\text{ZZ3}+5$. This is indeed what we obtain, as shown in Table I. Further, Table I shows a clear correlation between energy and band gap for the alloy structures. Note that the insulating $\text{A}_1\text{ZZ4}$ alloy has a lower energy than the $\text{A}_4\text{ZZ3}+5$.

In summary, the authors introduce a geometry for ultrathin Au, Ag, and Au-Ag-alloy wires that is more stable than previously considered planar geometries for these systems, by about 0.1 eV per atom. The insulating nature of this structure, with gaps of 1.3 eV for Au and 0.8 eV for Ag, is not related to Peierls instabilities, resulting, rather, from an interplay between geometric and electronic structure effects.

The authors acknowledge support from the Brazilian agencies: FAPEMIG, CAPES, CNPq, and Instituto de Milênio de Nanotecnologia/MCT.

-
- [1] H. Ohnishi, Y. Kondo, and K. Takayanagi, *Nature (London)* **395**, 780 (1998).
 - [2] A. I. Yanson, G. Rubio-Bollinger, H. E. van den Brom, N. Agrit, and J. M. van Ruitenbeek, *Nature (London)* **395**, 783 (1998).
 - [3] J. Bettini, F. Sato, P. Z. Coura, S. O. Dantas, D. S. Galvão, and D. Ugarte, *Nature Nanotechnology* **1**, 182 (2006).
 - [4] L. G. C. Rego, A. R. Rocha, V. Rodrigues, and D. Ugarte, *Phys. Rev. B* **67**, Art. No. 045412 (2003).
 - [5] V. Rodrigues, J. Bettini, A. R. Rocha, L. G. C. Rego, and D. Ugarte, *Phys. Rev. B* **65**, Art. No. 153402 (2002).
 - [6] L. Q. Ke, M. van Schilfgaarde, T. Kotani, and P. A. Bennett, *Nanotechnology* **18**, Art. No. 095709 (2007).
 - [7] A. Enomoto, S. Kurokawa, and A. Sakai, *Phys. Rev. B* **65**, Art. No. 125410 (2002).
 - [8] M. Springborg and P. Sarkar, *Phys. Rev. B* **68**, 045430 (2003).
 - [9] A. M. Asaduzzaman and M. Springborg, *Phys. Rev. B* **72**, 165422 (2005).
 - [10] F. J. Ribeiro and M. L. Cohen, *Phys. Rev. B* **68**, 035423 (2003).
 - [11] S. R. Bahn and K. W. Jacobsen, *Phys. Rev. Lett.* **87**, 266101 (2001).
 - [12] D. Sánchez-Portal, E. Artacho, J. Junquera, P. Ordejón, A. García, and J. M. Soler, *Rev. Lett.* **83**, 3884 (1999).
 - [13] R. H. M. Smit, C. Untiedt, A. I. Yanson, and J. M. van Ruitenbeek, *Phys. Rev. Lett.* **87**, 266102 (2001).
 - [14] I. P. Batra, *Phys. Rev. B* **42**, 9162 (1990).

- [15] D. Cheng, W. Y. Kim, S. K. Min, T. Nautiyal, and K. S. Kim, *Phys. Rev. Lett.* **96**, Art. No. 096104, 2006.
- [16] J. M. Soler, E. Artacho, J. D. Gale, A. Garcia, J. Junquera, P. Ordejon, and D. Sanchez-Portal, *J. Phys-Condens. Mat.* **14**, 2745 (2002).
- [17] W. Kohn, L. J. Sham. *Phys. Rev.* **140**, A1133 (1965).
- [18] J. P. Perdew, K. Burke, and M. Ernzerhof, *Phys. Rev. Lett.* **77**, 3865 (1996).
- [19] N. Troullier and J. L. Martins, *Phys. Rev. B* **43**, 1993 (1991).